Proceedings of the
46th IEEE Conference on Decision and Control
New Orleans, LA, USA, Dec. 12-14, 2007

A Delay-Duhem Model for Jump-Resonance Hysteresis*

Ashwani K. Padthe and Dennis S. Bernstein
Department of Aerospace Engineering, The University of Michigan,
Ann Arbor, MI 48109-2140, USA, {akpadthe,dsbaero}@umich.edu

Abstract— **In this paper we present a Duhem hysteretic model that models jump resonance hysteresis in Duffing's oscillator. In order to obtain the Duhem model, we use a nonlinear oscillator that can output a harmonic signal of specified frequency and amplitude. We also use a sliding time averaging system that captures the mean square value of a variable-period signal. The presented Duhem model represents the excitation frequency versus response amplitude hysteresis of Duffing's oscillator in the sense of a persistent input-output loop under asymptotically slow periodic excitation. We also show that the jump resonance hysteresis is rate dependent.**

I. Introduction

Hysteresis is an intrinsically nonlinear phenomenon that manifests itself as a nontrivial input-output loop (the hysteresis map) that persists at asymptotically slow periodic excitation. In effect, the asymptotic input-output loop is a quasi-DC vestige of the dynamic characteristics of a system [1].

When the input is force and the output is displacement, the area enclosed by a hysteresis loop is equal to the energy dissipated during one cycle of periodic excitation. A linear system with viscous damping is not hysteretic due to the fact that no energy is dissipated in the limit of DC operation; indeed, at low-frequency excitation, the input-output loop collapses, and the asymptotic loop area is zero. However, nonlinear friction models as well as hysteretically damped structures exhibit persistent energy dissipation even as the rate of excitation converges to zero [2].

A definition of hysteresis must recognize the distinction between the limiting hysteresis map and the natural dynamics of the system. Logic hysteresis maps as well as some ferromagnetic models have the property that the periodic input-output loop is identical for all frequencies of excitation; such systems possess *rate-independent hysteresis*. Mechanical systems, which possess inertia and thus resonance, exhibit dynamics that are sensitive to the frequency of excitation; such systems can possess *rate-dependent hysteresis*. This distinction is discussed in [1]. It is important to stress, however, that hysteresis per se refers to the persistent quasi-DC input-output loop.

From a system-theoretic perspective, hysteresis is a consequence of *multistability*, that is, the existence of multiple attracting input-dependent equilibria, where "input dependent" refers to the equilibria possessed by the system for a given constant input value. Under asymptotically slow excitation, the state of the system converges to the equilibria corresponding to the current value of the input, thus giving rise to the hysteresis map. The simplest situation is that of *bifurcation hysteresis* as exhibited by the cubic feedback model in [3]. In this case, the system may possess one, two, or three equilibria, some of which may be attractive and some of which are unstable, while not all are present for all input values. A related, but more complex, situation involves the freeplay or backlash model, in which case the deadzone nonlinearity gives rise to a continuum of equilibria. Both of these models involve a linear system with nonlinear feedback [4].

An alternative finite-dimensional model exhibiting hysteresis is the Duhem model. These models are widely used to model friction phenomena [2], [5]–[13] as well as ferromagnetism [14]–[16]. Infinite-dimensional models of hysteresis include superposition models such as the Preisach and related integral operator models [17]–[21]. Unlike the Duhem model, Preisach models exhibit nonlocal memory, which manifests itself upon input reversal [20].

The present paper focuses on a widely studied hysteretic phenomenon that has not been linked to either nonlinear feedback, Duhem, or superposition models. In particular, we consider jump resonance in nonlinear oscillators subject to swept harmonic forcing. To illustrate jump resonance we briefly review the classical analysis [22]–[24]. Consider Duffing's oscillator

$$\ddot{z} + 2\beta\omega_0\dot{z} + \omega_0^2 z + \gamma z^3 = A\sin(\Omega t), \tag{1}$$

where ω_0 is the undamped linear natural frequency, β is the damping ratio, γ is the coefficient of the cubic nonlinearity, and A and Ω are the amplitude and frequency, respectively, of the external harmonic excitation.

To analyze jump resonance, we make the approximating assumption that the response of (1) is harmonic with frequency Ω, that is, $z(t) \approx Z\sin(\Omega t)$. Approximate solutions to Duffing's equation are obtained assuming that γ, β, and A are small [22]. Under these assumptions, the input frequency Ω and output amplitude Z are related by

$$\tfrac{9}{16}\gamma^2(Z^2)^3 - 3(\Omega-\omega_0)\omega_0\gamma(Z^2)^2 + 4\omega_0^2[\omega_0^2\beta^2 + (\Omega-\omega_0)^2]Z^2 - A^2 = 0. \tag{2}$$

Figure 1, which is based on equation (2), shows the relationship between Z and Ω for $A = 0.2$, $\omega_0 = 1$, $\beta = 0.05$, and $\gamma = 0.5$. Note that (2) is a third order polynomial in Z^2 and hence, indicates the existence of three output

*This research was supported in part by the National Science Foundation under grant ECS–0225799.

amplitudes (considering only the positive values of Z) at certain frequencies Ω. Also, it has been observed that one of the three amplitude values is unstable leading to the jump phenomenon.

To demonstrate jump resonance in (1) the input frequency Ω is not held constant, but rather is swept slowly between two specified frequencies, say, Ω_1 and Ω_2. Letting $\Omega_1 = 0.8$ rad/s and $\Omega_2 = 2.2$ rad/s, (1) is simulated with the slowly time-varying frequency $\Omega(t) = 1.5 + 0.7\sin(0.001t)$ rad/s, and the response is shown in Figure 2. Note that the variation in the peak value of $z(t)$ in Figure 2 corresponds to the variation of the response amplitude Z in Figure 1. There is a considerable difference between the peak amplitude values obtained through actual simulations of Duffing's equation and approximate analytical solutions.

Despite the obvious hysteretic nature of Duffing's oscillator under swept harmonic forcing, the relationship between this hysteretic behavior and standard hysteresis models has not been demonstrated. Consequently, the objective of this paper is to derive a dynamic model that exhibits hysteresis in the sense of a persistent input-output loop under asymptotically slow periodic excitation. In fact, the approximate analysis shown in Figure 1 does not constitute a hysteresis map in the usual sense since the input to the system is a harmonic signal and the output is the peak value of a periodic signal.

To obtain a dynamical system that captures jump resonance, we combine three elements, as shown in Figure 3. The first element is an autonomous nonlinear dynamical system that has the property that, given frequency and amplitude parameters, the state converges to a harmonic signal with the specified amplitude and frequency. This system is a variation of the van der Pol oscillator with the crucial difference being that the limit cycle is harmonic. We call this system the *Roup oscillator* for its originator [25], [26].

Next, we slowly sweep the frequency parameter of the Roup oscillator in order to generate an approximate harmonic sweep given by the state of the Roup oscillator. Note that the only input to the system is the swept frequency, and not a harmonic signal per se. We then use the response of the Roup oscillator as the input to Duffing's oscillator.

Although the hysteretic response of Duffing's oscillator is manifested in the peak amplitude of its approximately harmonic response, the peak amplitude cannot be obtained by appending an output function. Consequently, we employ an averaging technique to approximate the mean square value of the output. Since this value must be obtained under harmonically swept excitation, we use a variable-period *sliding average* in which the averaging period is given by the frequency parameter for the Roup oscillator.

Finally, we differentiate the output of the sliding average operator to obtain a differential equation for the combined system. The resulting system, comprised of the Roup oscillator, Duffing's equation, and sliding-average operator, is 5^{th}-order. This 5^{th}-order system is a Duhem model with a delay in one of the states due to the averaging operator.

In Section 2 we briefly summarize some terminology and

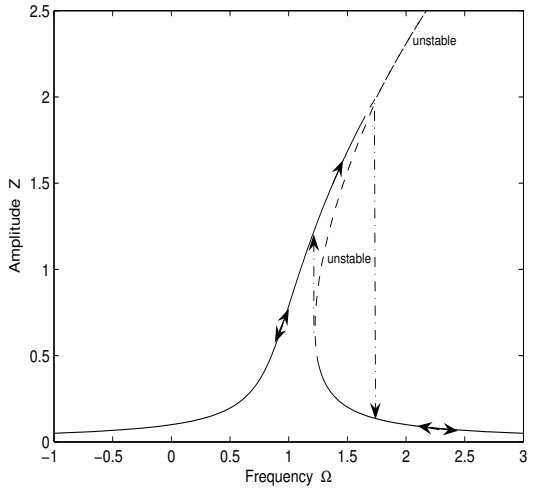

Fig. 1. Resonance curve given by (2) for Duffing's oscillator (1) showing hysteresis between the response amplitude Z and excitation frequency Ω. The parameters used are $A = 0.2$, $\omega_0 = 1$, $\beta = 0.05$, and $\gamma = 0.5$.

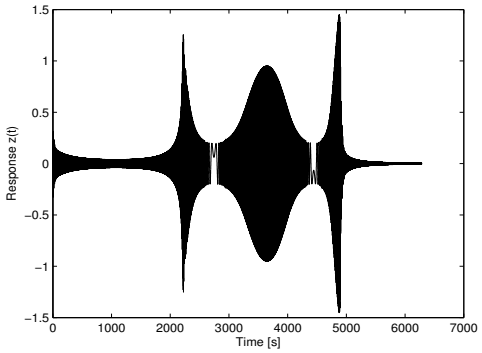

Fig. 2. Response $z(t)$ of Duffing's oscillator (1) for an excitation with time-varying frequency given by $\Omega(t) = 1.5 + 0.7\sin(0.001t)$ rad/s. The parameters used are $A = 0.2$, $\omega_0 = 1$, $\beta = 0.05$, and $\gamma = 0.5$.

basic results concerning Duhem models. Next, in Section 3, we describe the Roup oscillator and summarize its asymptotic properties. Section 4 presents the sliding-average operator, while the Roup oscillator, Duffing's equation, and the sliding-average operator are combined in Section 5.

II. Generalized Duhem Models

In this section, we summarize the main results of [1] concerning the generalized and semilinear Duhem models. Consider the single-input, single-output *generalized Duhem model*

$$\dot{x}(t) = f\big(x(t), u(t)\big)g\big(\dot{u}(t)\big), \qquad x(0) = x_0, \quad t \geq 0, \tag{3}$$

$$y(t) = h\big(x(t), u(t)\big), \tag{4}$$

where $x : [0, \infty) \to \mathbb{R}^n$ is absolutely continuous, $u : [0, \infty) \to \mathbb{R}$ is continuous and piecewise C^1, $f : \mathbb{R}^n \times \mathbb{R} \to \mathbb{R}^{n\times r}$ is continuous, $g : \mathbb{R} \to \mathbb{R}^r$ is continuous and satisfies $g(0) = 0$, and $y : [0, \infty) \to \mathbb{R}$, and $h : \mathbb{R}^n \times \mathbb{R} \to \mathbb{R}$ are continuous. The value of $\dot{x}(t)$ at a point t at which

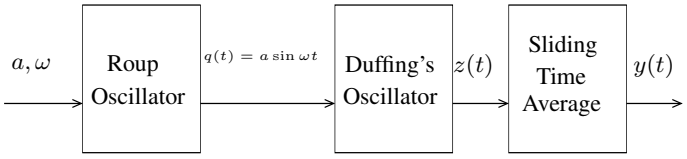

Fig. 3. Block diagram showing the interconnection of the components used to generate a Duhem hysteretic model for jump-resonance.

$\dot{u}(t)$ does not exist can be assigned arbitrarily. We assume that the solution to (3) exists and is unique on all finite intervals. Under these assumptions, x and y are continuous and piecewise C^1. The terms closed curve, limiting periodic input-output map, hysteresis map, and rate independence are defined as follows.

Definition 2.1: The nonempty set $\mathcal{H} \subset \mathbb{R}^2$ is a *closed curve* if there exists a continuous, piecewise C^1, and periodic map $\gamma : [0, \infty) \to \mathbb{R}^2$ such that $\gamma([0, \infty)) = \mathcal{H}$.

Definition 2.2: Let $u : [0, \infty] \to [u_{\min}, u_{\max}]$ be continuous, piecewise C^1, periodic with period α, and have exactly one local maximum $u_{\max}$ in $[0, \alpha)$ and exactly one local minimum $u_{\min}$ in $[0, \alpha)$. For all $T > 0$, define $u_T(t) \triangleq u(\alpha t/T)$, assume that there exists $x_T : [0, \infty) \to \mathbb{R}^n$ that is periodic with period T and satisfies (3) with $u = u_T$, and let $y_T : [0, \infty) \to \mathbb{R}$ be given by (4) with $x = x_T$ and $u = u_T$. For all $T > 0$, the *periodic input-output map* $\mathcal{H}_T(u_T, y_T)$ is the closed curve $\mathcal{H}_T(u_T, y_T) \triangleq \{\big(u_T(t), y_T(t)\big) : t \in [0, \infty)\}$, and the *limiting periodic input-output map* $\mathcal{H}_\infty(u)$ is the closed curve $\mathcal{H}_\infty(u) \triangleq \lim_{T\to\infty} \mathcal{H}_T(u_T, y_T)$ if the limit exists. If there exist $(u, y_1), (u, y_2) \in \mathcal{H}_\infty(u)$ such that $y_1 \neq y_2$, then $\mathcal{H}_\infty(u)$ is a *hysteresis map*, and the generalized Duhem model is *hysteretic*.

Definition 2.3: The continuous and piecewise C^1 function $\tau : [0, \infty) \to [0, \infty)$ is a *positive time scale* if $\tau(0) = 0$, τ is nondecreasing, and $\lim_{t\to\infty} \tau(t) = \infty$. The generalized Duhem model (3), (4) is *rate independent* if, for every pair of continuous and piecewise C^1 functions x and u satisfying (3) and for every positive time scale τ, it follows that $x_\tau(t) \triangleq x(\tau(t))$ and $u_\tau(t) \triangleq u(\tau(t))$ also satisfy (3).

The following result is proved in [1].

Proposition 2.1: Assume that g is positively homogeneous, that is, $g(\alpha v) = \alpha g(v)$ for all $\alpha > 0$ and $v \in \mathbb{R}$. Then the generalized Duhem model (3), (4) is rate independent.

If g is positively homogeneous, then there exist $h_+, h_- \in \mathbb{R}^r$ such that

$$g(v) = \begin{cases} h_+ v, & v \geq 0, \\ h_- v, & v < 0, \end{cases} \tag{5}$$

and the rate-independent generalized Duhem model (3), (4) can be reparameterized in terms of u [1]. Specifically, consider

$$\frac{\mathrm{d}\hat{x}(u)}{\mathrm{d}u} = \begin{cases} f_+(\hat{x}(u), u), & \text{when } u \text{ increases}, \\ f_-(\hat{x}(u), u), & \text{when } u \text{ decreases}, \\ 0, & \text{otherwise}, \end{cases} \tag{6}$$

$$\hat{y}(u) = h\big(\hat{x}(u), u\big), \tag{7}$$

for $u \in [u_{\min}, u_{\max}]$ and with initial condition $\hat{x}(u_0) = x_0$, where $f_+(x, u) \triangleq f(x, u)h_+$, $f_-(x, u) \triangleq f(x, u)h_-$, and $u_0 \in [u_{\min}, u_{\max}]$. Then $x(t) \triangleq \hat{x}(u(t))$ and $y(t) \triangleq \hat{y}(u(t))$ satisfy (3), (4). Note that the reparameterized Duhem model (6) and (7) can be viewed as a time-varying dynamical system with nonmonotonic time u.

III. A Nonlinear System for Generating Sinusoidal Signals

In order to obtain hysteresis for which the input variable is frequency, we require a time-invariant system that generates a sinusoidal signal of specified frequency and amplitude. We thus consider the Roup oscillator

$$\ddot{q} + \lambda(q^2 + \frac{1}{\omega^2}\dot{q}^2 - a^2)\dot{q} + \omega^2 q = 0, \tag{8}$$

where a, ω, and λ are positive constants. Note that a solution of (8) is given by

$$q(t) = a \sin(\omega t). \tag{9}$$

The following result shows that, for all nonzero initial conditions, the solution of (8) approaches (9).

Proposition 3.1: Let q satisfy (8). Then $\lim_{t\to\infty}[q(t) - a\sin(\omega t)] = 0$ for all nonzero initial conditions $q(0)$, $\dot{q}(0)$.

Proof: The proof is based on Example 2.9 of [27] which proves the existence of a stable limit cycle for the Van der Pol oscillator. First we define $x_1 = q$, $x_2 = \dot{q}$, and rewrite (8) in the state-space form

$$\dot{x}_1 = x_2, \tag{10}$$

$$\dot{x}_2 = -\lambda(x_1^2 + \frac{1}{\omega^2}x_2^2 - a^2)x_2 - \omega^2 x_1. \tag{11}$$

The system (10), (11) has a unique equilibrium point at the origin. Using similar arguments and the Lyapunov like function $V(x_1, x_2) = \frac{1}{2}\left(x_1^2 + \frac{x_2^2}{\omega^2}\right)$ as given in the Example 2.9 of [27], it can be shown that there exists a closed, bounded region M in the phase plane of the system (10), (11) such that all the trajectories originating in M at $t = 0$ remain in M for all $t > 0$. The derivative of $V(x_1, x_2)$ is given by

$$\begin{aligned} \dot{V}(x_1, x_2) &= x_1\dot{x}_1 + \frac{1}{\omega^2}x_2\dot{x}_2 \\ &= x_1 x_2 + \frac{1}{\omega^2}x_2(-\lambda(x_1^2 + \frac{1}{\omega^2}x_2^2 - a^2)x_2 - \omega^2 x_1) \\ &= -\frac{\lambda}{\omega^2}(x_1^2 + \frac{1}{\omega^2}x_2^2 - a^2)x_2^2. \end{aligned} \tag{12}$$

Note that the term $x_1^2 + \frac{1}{\omega^2}x_2^2 - a^2$ in (12) represents an ellipse E. Hence, $\dot{V}$ is positive for all the points inside the ellipse and negative for all the points outside the ellipse. This ellipse is analogous to the region $0 < x_1 < a$ in the Example 2.9 of [27]. So we have a closed, bounded region that has only one equilibrium point at the origin. The Jacobian matrix at the origin

$$J(0, 0) = \begin{bmatrix} 0 & 1 \\ -\omega^2 & \lambda a^2 \end{bmatrix} \tag{13}$$

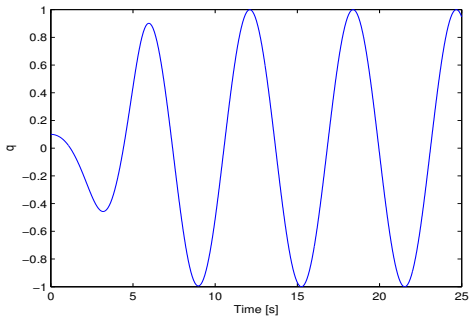

(a)

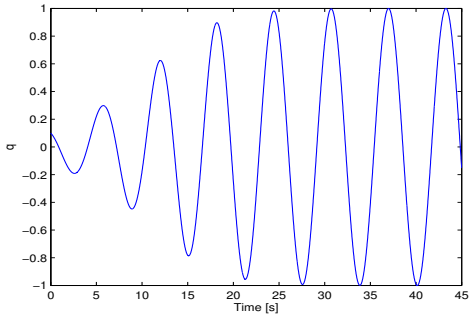

(b)

Fig. 4. The response $q(t)$ of the system (8) with (a) $\lambda = 1$, (b) $\lambda = 0.3$. The parameters used are $a = 1$, $\omega = 1$ and the initial conditions are $q(0) = .1,\ \dot{q}(0) = .1$.

has eigenvalues $\frac{1}{2}(\lambda a^2 \pm \sqrt{\lambda a^2 - 4\omega^2})$. At least one of the eigenvalues is unstable for all values of a, λ, and ω. Hence, by the Poincare-Bendixson criterion, we conclude that there exists a closed periodic orbit in the region M.

Note that $\dot{V}(x_1, x_2) = 0$ on the ellipse E. Using this fact and arguments from [27], pp. 65, it can be shown that the system (10), (11) has a unique closed periodic orbit given by

$$x_1^2 + \frac{1}{\omega^2} x_2^2 - a^2 = 0, \tag{14}$$

which corresponds to the harmonic solution given by (9).

Finally, it can be shown using arguments from [27], pp. 66, that all the trajectories in the phase plane converge to the closed orbit given by (14). ■

The nonlinear oscillator (8) is analogous to the Van der Pol oscillator since both equations have a stable limit cycle. The distinction between the Van der Pol oscillator and the Roup oscillator is that in the later case the limit cycle is a harmonic signal of specified frequency and amplitude and hence, is known analytically, namely, given by (9). The parameter λ in (8) determines the speed of convergence to the steady state solution. A higher value of λ implies faster convergence. Using the values $a = 1$, $\omega = 1$ and initial conditions $q(0) = 1$, $\dot{q}(0) = 1$, the response $q(t)$ for $\lambda = 1$ and $\lambda = 0.3$ is shown in Figures 4(a) and 4(b), respectively.

IV. Sliding Time Average of a Periodic Signal

As shown in Figure 1, Duffing's oscillator exhibits hysteresis between the response amplitude and the input frequency. In the absence of a function that can extract the amplitude of a periodic signal, we alternatively use a sliding time average of an approximately periodic signal with slowly time-varying period $\frac{2\pi}{u(t)}$, defined as

$$y(t) \triangleq \frac{u(t)}{2\pi} \int_{t-\frac{2\pi}{u(t)}}^{t} z^2(\tau) \mathrm{d}\tau. \tag{15}$$

Differentiating (15) and using the Leibniz's integral rule we have

$$\begin{aligned} \dot{y}(t) = \frac{u(t)}{2\pi} \left[z^2(t) - z^2(t - \frac{2\pi}{u(t)}) \left[1 + \frac{2\pi \dot{u}(t)}{u^2(t)} \right] \right] \\ + \frac{\dot{u}(t)}{2\pi} \int_{t-\frac{2\pi}{u(t)}}^{t} z^2(\tau) \mathrm{d}\tau. \end{aligned} \tag{16}$$

Now substituting (15) in (16) we obtain

$$\begin{aligned} \dot{y}(t) = \frac{u(t)}{2\pi} \left[z^2(t) - z^2(t - \frac{2\pi}{u(t)}) \left[1 + \frac{2\pi \dot{u}(t)}{u^2(t)} \right] \right] \\ + \frac{y(t)}{u(t)} \dot{u}(t), \end{aligned} \tag{17}$$

which upon rearranging yields,

$$\begin{aligned} \dot{y}(t) = \left[z^2(t) - z^2(t - \frac{2\pi}{u(t)}) \right] \frac{u(t)}{2\pi} \\ - \frac{z^2(t - \frac{2\pi}{u(t)})}{u(t)} \dot{u}(t) + \frac{y(t)}{u(t)} \dot{u}(t). \end{aligned} \tag{18}$$

We do not take the square root of the output in order to preserve the continuity of the 5^{th}-order system given in the next section. Trends in the output variation can be extracted working with the square of the output.

V. Duhem Model for Hysteresis in Jump Resonance

We now combine (8), (1), and (18) into a system of 5 first-order differential equations given by

$$\dot{x}_1 = x_2, \tag{19}$$

$$\dot{x}_2 = -\lambda \left(x_1^2 + \frac{1}{u^2} x_2^2 - a^2 \right) x_2 - u^2 x_1, \tag{20}$$

$$\dot{x}_3 = x_4, \tag{21}$$

$$\dot{x}_4 = -2\beta\omega_0 x_4 - \omega_0^2 x_3 - \gamma x_3^3 + x_1, \tag{22}$$

$$\dot{x}_5 = \left[x_3^2 - (\delta_{2\pi/u} x_3)^2 \right] \frac{u}{2\pi} - \left[(\delta_{2\pi/u} x_3)^2 - x_5 \right] \frac{\dot{u}}{u}, \tag{23}$$

where $x_1 \triangleq q$, $x_2 \triangleq \dot{q}$, $x_3 \triangleq z$, $x_4 \triangleq \dot{z}$, $x_5 \triangleq y$, $u \triangleq \omega$, and $\delta_{2\pi/u} x_3 = x_3(t - \frac{2\pi}{u})$. Note that the equations (19), (20) are derived from (8) and the equations (21), (22) are derived from (1). The input frequency ω in (8) is represented as the input u for the system of equations (19)-(23). For a constant input $u = u_0$, $\lim_{t\to\infty}(x_1(t) - a\sin(u_0 t)) \to 0$ and the sinusoidal signal $x_1(t) = a\sin(u_0 t)$ is fed as the harmonic excitation to the first-order Duffing's equations (21), (22). The interconnection between the various systems is shown in the Figure 3.

Equations (19)-(23) can be rewritten as

$$\dot{x} = f(x,u)g(\dot{u}), \tag{24}$$

$$y = h(x), \tag{25}$$

where

$$x = \begin{bmatrix} x_1 \\ x_2 \\ x_3 \\ x_4 \\ x_5 \end{bmatrix}, g(\dot{u}) = \begin{bmatrix} 1 \\ \dot{u} \end{bmatrix}, h(x) = x_5, \tag{26}$$

$$f(x,u) = \begin{bmatrix} x_2 & 0 \\ -\lambda\left(x_1^2+\frac{1}{u^2}x_2^2-a^2\right)x_2-u^2x_1 & 0 \\ x_4 & 0 \\ -2\beta\omega_0 x_4-\omega_0^2 x_3-\gamma x_3^3+x_1 & 0 \\ \left[x_3^2-(\delta_{2\pi/u}x_3)^2\right]\frac{u}{2\pi} & -\left[(\delta_{2\pi/u}x_3)^2-x_5\right]\frac{1}{u} \end{bmatrix}, \tag{27}$$

which is a generalized Duhem model of the form (3), (4) except the lag term $\delta_{2\pi/u}x_3$. Note that the output $y = x_5$ is the sliding time average of the periodic response from the first-order Duffing's equations (21), (22) and the input u is the frequency of the harmonic excitation x_1 given to the first-order Duffing's equations (21), (22). It was shown in the introduction that there exists hysteresis between the amplitude of the response and the frequency of the harmonic excitation given to Duffing's equation (1).

We now present results from simulations of (24), (25). Let the input $u(t) = 1.5 + 1.2\sin(0.001t)$. Then x_1 is a sinusoid with a constant amplitude and a time-varying frequency given by $u(t)$. The input $u(t)$ affects x_3 and x_4 through x_1. Time history of the state $x_3(t)$ is shown in the Figure 5(a). The hysteresis map between the output $y(t)$ which is the running time average of $x_3(t)$ and the input $u(t)$ is shown in the Figure 5(b). Figures 6, 7(a), and 7(b) show the input, x_3, and the hysteresis map, respectively for a triangular shaped input.

The hysteretic Duhem model (24), (25) is rate-dependent since the function $g(\dot{u})$ is not positively homogeneous [1]. A rate-dependent hysteretic model gives a different hysteresis loop for different shapes and frequencies of the periodic input. Figure 8 shows hysteresis maps for a sinusoidal and a triangular input together. Note that the two hysteresis maps are different, thus, confirming the rate-dependence of the Duhem model (24), (25).

VI. Conclusion

In this paper we modeled the classical jump resonance hysteresis in Duffing's oscillator as a generalized Duhem hysteretic model. We presented a nonlinear oscillator that can generate a harmonic signal of specified frequency and amplitude. The Duhem model helps in representing the jump resonance hysteresis as the conventional input-output hysteresis. Using the Duhem model we also show that the jump resonance hysteresis is rate-dependent.

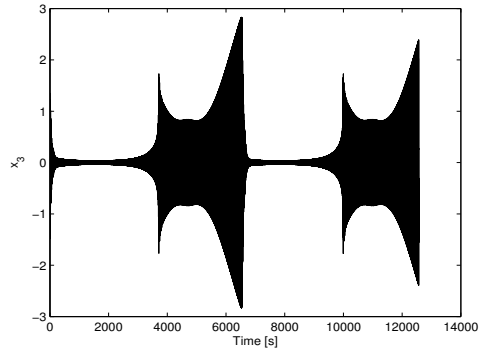

(a)

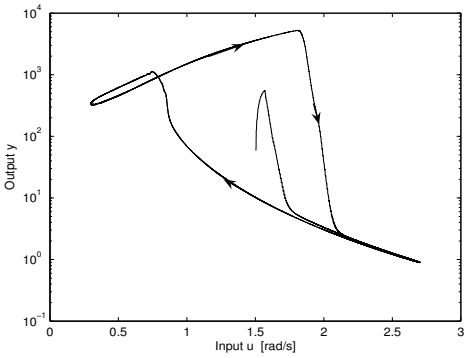

(b)

Fig. 5. (a) Time history of the state $x_3(t)$ of the system (24), (25), (b) Hysteresis map between the output $y(t)$ which is the running time average of $x_3(t)$ and the input $u(t)$ of the system (24), (25), for $u(t) = 1.2\sin(0.001t) + 1.5$ rad/s. Note that $u(t)$ affects the states $x_3(t)$ and $x_4(t)$ through $x_1(t)$. The parameters used are $a = 0.25$, $\lambda = 1$, $\omega_0 = 0.5$, $\beta = 0.05$, $\gamma = 0.5$, and the initial conditions are $[x_1(0)\ x_2(0)\ x_3(0)\ x_4(0)\ x_5(0)]' = [1\ 1\ 0\ 0\ 0]'$.

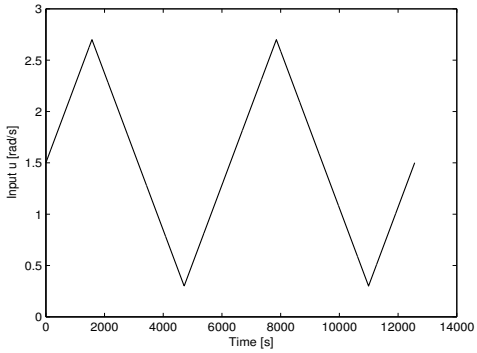

Fig. 6. Triangular input given to the system (24), (25).

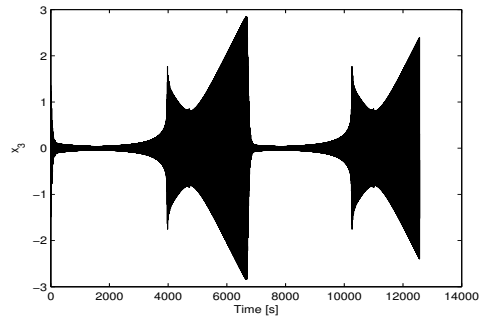

(a)

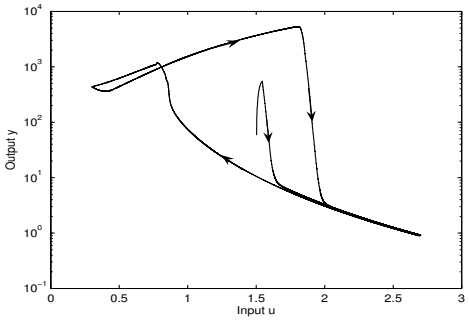

(b)

Fig. 7. (a) Time history of the state $x_3(t)$ of the system (24), (25), (b) Hysteresis map between the output $y(t)$ which is the running time average of $x_3(t)$ and the input $u(t)$ of the system (24), (25), for a triangular input $u(t)$. Note that $u(t)$ affects the states $x_3(t)$ and $x_4(t)$ through $x_1(t)$. The parameters used are $a = 0.25$, $\lambda = 1$, $\omega_0 = 0.5$, $\beta = 0.05$, $\gamma = 0.5$, and the initial conditions are $[x_1(0)\ x_2(0)\ x_3(0)\ x_4(0)\ x_5(0)]' = [1\ 1\ 0\ 0\ 0]'$.

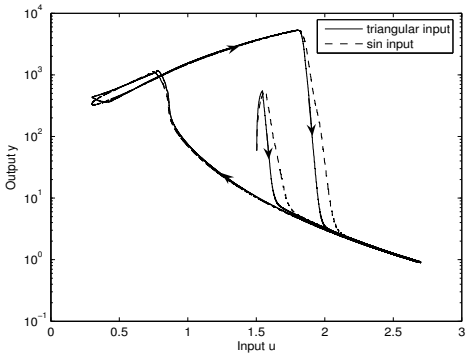

Fig. 8. Hysteresis maps for the system (24), (25) with sinusoidal and triangular inputs . The two hysteresis maps are different, thus, confirming the rate-dependence of the Duhem model (24), (25).

Acknowledgement

We wish to thank Steve Shaw for suggesting the connection between jump-resonance hysteresis and Duhem models.

REFERENCES

[1] J. Oh and D. S. Bernstein, "Semilinear Duhem model for rate-independent and rate-dependent hysteresis," *IEEE Trans. Autom. Contr.*, vol. 50, pp. 631–645, 2005.

[2] A. Padthe, J. Oh, and D. S. Bernstein, "On the lugre model and friction-induced hysteresis," in *Proc. Amer. Contr. Conf.*, Minneapolis, MN, June 2006, pp. 3247–3252.

[3] J. K. Hale and H. Koçak, *Dynamics and Bifurcations*. New York: Springer-Verlag, 1991.

[4] J. Oh and D. S. Bernstein, "Step-convergence analysis of nonlinear feedback hysteresis models," in *Proc. Amer. Contr. Conf.*, Portland, OR, June 2005, pp. 697–702.

[5] J. Oh, A. Padthe, D. S. Bernstein, D. Rizos, and S. D. Fassois, "Duhem models for hysteresis in sliding and presliding friction," in *Proc. IEEE Conf. Dec. Contr.*, Seville, Spain, December 2005, pp. 8132–8137.

[6] A. Padthe and D. S. Bernstein, "Duhem feedback and friction-induced staircase hysteresis," in *Proc. Amer. Contr. Conf.*, New York, NY, July 2007, submitted.

[7] P. Dahl, "Solid friction damping of mechanical vibrations," *AIAA J.*, vol. 14, no. 2, pp. 1675–82, 1976.

[8] D. D. Rizos and S. D. Fassois, "Presliding friction identification based upon the Maxwell slip model structure," *Chaos*, vol. 14, no. 2, pp. 431–445, 2004.

[9] C. Canudas de Wit, H. Olsson, K. J. Åstrom, and P. Lischinsky, "A new model for control of systems with friction," *TAC*, vol. 40, no. 3, pp. 419–425, 1995.

[10] J. Swevers, F. Al-Bender, C. G. Ganseman, and T. Prajogo, "An integrated friction model structure with improved presliding behavior for accurate friction compensation," *IEEE Trans. Autom. Contr.*, vol. 45, no. 4, pp. 675–686, 2000.

[11] B. Armstrong-Hélouvry, P. Dupont, and C. C. de Wit, "A survey of model, analysis tools and compensation methods for the control of machines with friction," *Automatica*, vol. 30, no. 7, pp. 1083–1138, 1994.

[12] F. Al-Bender, V. Lampaert, and J. Swevers, "Modeling of dry sliding friction dynamics: From heuristic models to physically motivated models and back," *Chaos*, vol. 14, no. 2, pp. 446–445, 2004.

[13] F. Al-Bender, V. Lampaert, S. D. Fassois, D. D. Rizos, K. Worden, D. Engster, A. Hornstein, and U. Parlitz, "Measurement and identification of pre-sliding friction dynamics," in *Nonlinear Dynamics of Production Systems*. Weinheim: Wiley, 2004, pp. 349–367.

[14] B. D. Coleman and M. L. Hodgdon, "A constitutive relation for rate-independent hysteresis in ferromagnetically soft materials," *Int. J. Eng. Sci.*, vol. 24, pp. 897–919, 1986.

[15] M. L. Hodgdon, "Applications of a theory of ferromagnetic hysteresis," *IEEE Trans. Magnetics*, vol. 24, pp. 218–221, 1988.

[16] ——, "Mathematical theory and calculations of magnetic hysteresis curves," *IEEE Trans. Magnetics*, vol. 24, pp. 3120–3122, 1988.

[17] A. Visintin, *Differential Models of Hysteresis*. New York: Springer-Verlag, 1994.

[18] ——, "On the Preisach model for hysteresis," *Nonlinear Analysis, Theory, Methods and Application*, vol. 8, no. 9, pp. 977–996, 1984.

[19] M. Brokate and A. Visintin, "Properties of the Preisach model for hysteresis," *J. Reineund Angewandte Mathematik*, vol. 402, pp. 1–40, 1989.

[20] I. D. Mayergoyz, *Mathematical Models of Hysteresis*. New York: Springer-Verlag, 1991.

[21] R. B. Gorbet, K. A. Morris, and D. W. L. Wang, "Control of hysteretic systems: A state space approach," in *Learning, Control and Hybrid Systems*. New York: Springer, 1998, pp. 432–451.

[22] J. J. Thomsen, *Vibrations and Stability*. New York, NY: McGraw-Hill, 1997.

[23] F. C. Moon, *Chaotic Vibrations*. New York: Wiley, 1987.

[24] N. Minorsky, *Nonlinear Oscillations*. New York: Van Nostrand Reinhold, 1962.

[25] A. V. Roup and D. S. Bernstein, "Adaptive stabilization of a class of nonlinear systems with nonparametric uncertainty," *IEEE Trans. Autom. Contr.*, vol. 46, no. 11, pp. 1821–1825, 2001.

[26] S. L. Lacy and D. S. Bernstein, "Identification of systems with limit cycles," in *Proc. Amer. Contr. Conf.*, Denver, CO, June 2003, pp. 3863–3868.

[27] H. K. Khalil, *Nonlinear Systems*, 3rd ed. New York: Prentice Hall, 2002.